Application of Coupled Eulerian Lagrangian Approach in Finite Element Simulation of Friction Stir Welding

Sanjeev N K*, Ravikiran B P

Robert Bosch Engineering and Business Solutions Private Limited, Bangalore, India

*Sanjeev.NambihallyKumaraswamy@in.bosch.com

Abstract— *Finite Element Simulation of Friction Stir Welding (FSW) is a problem involving large deformations and is often difficult to solve using the classical Finite Element Method (FEM). Large mesh distortions and contact problems can occur due to the large deformations such that a convergent solution cannot be achieved. Since in ABAQUS, a Coupled Eulerian Lagrangian (CEL) approach has been developed to overcome the difficulties with regard to FEM and large deformation analyses. In this article, this method is investigated regarding its capabilities in simulating FSW process. FSW is a mechanical process whereby solid-state welding is performed using heat generated from the friction of a rotating tool and plastic deformation of weld material. FSW is a modification of the traditional Friction Welding, which was invented at the Welding Institute in Cambridge, England in 1991. Since then, it is gaining significance in many joining applications, by overcoming the limitations of other fusion welding processes. For successful incorporation of its potential during industrial applications, mechanism of joining needs to be properly comprehended. Various experimenting and study techniques are used in widening of its applicability in joining process. FE Simulation is one such technique which would help in getting an insight of the process phenomena during the process and the overall result could be used to observe the effect of process parameters on weld quality. Here, an attempt is made to develop a FE model using ABAQUS/Explicit with help of CEL formulation, Johnson-Cook material law and Coulomb's Law of friction. The model has been found to be capable of obtaining certain insight on right processing conditions prior to performing welding process, by predicting the effect of process parameters on outputs like temperature, force on tool and formation of defects. Finally the FE Simulation results are used to obtain the optimized process parameters.*

Keywords— *Friction Stir Welding, Finite Element Simulation, Coupled Eulerian Lagrangian, ABAQUS.*

1. Introduction

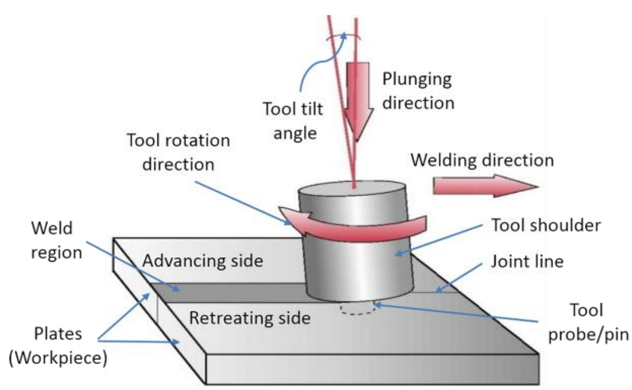

Figure 1. Schematic representation of friction stir welding process [1, 2]

Friction Stir Welding (FSW) is a solid-state joining process that uses a third body tool to join two facing surfaces. The welding of surfaces is achieved with the heat generated from the friction of a rotating tool and plastic deformation of weld material [3, 4]. Two metals that are to be welded together are held in place against a backing plate using a clamping system. The rotating tool is then slowly plunged with a downward force into the weld joint. It dwells for a few seconds while enough heat is generated due to friction that the material to be welded begins to flow around the tool. Once this point is reached, the tool is traversed along the joint forming the weld behind the tool as it moves along [5, 6]. The schematic representation of FSW is depicted in Figure 1. The main benefit of friction stir welding is that the pieces to be welded would not be reaching their melting points [7, 8].

The FSW process offers significant advantages as compared with fusion joining processes for aluminum, several of which are particularly important to the aerospace and automotive industry. These advantages include improved joint efficiency (tensile strength), improved fatigue life, no need for consumables and improved process robustness. Since from its invention, it has rapidly evolved and has opened up a variety of research channels. It is being touted as the most significant development in metal joining in the last decade [3, 4]. Many alloys, including most aerospace Al alloys (e.g., Al 7xxx) and those regarded as difficult to weld by fusion processes (e.g., Al 2xxx), may be welded by FSW [9].

2. Objective of the work

FSW presents a multiphysics modeling challenge, because it combines closely coupled heat flow, plastic deformation at high temperature and microstructure and property evolution. All three contribute to the process-ability of a material by FSW and to the subsequent properties of the weld.**Figure*2*** illustrates the key physical interactions involved in FSW process and to the outputs needed by designers. But the bottle neck experienced in FSW is fixing the right processing parameters when a certain job arrives on the shop floor, parameters change with thickness of job and material of job. Here the main object is to get the parameters at which the weld can be performed for selected material and thickness with in the stipulated time.

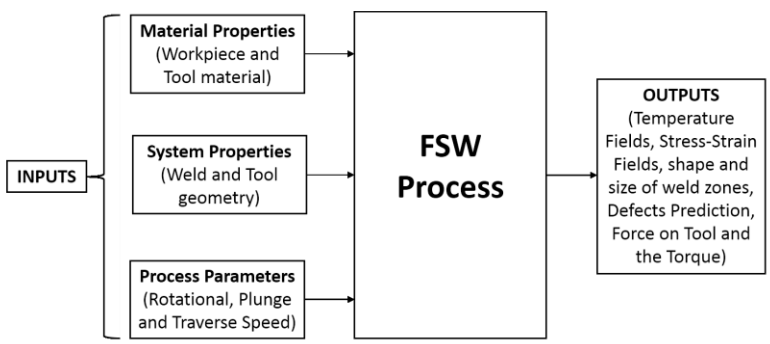

Figure2. Summary of interactions in FSW process

3. Approach and Actual Work Done

In literature, the existing method i.e., Experimental-based approach used for obtaining optimal process parameters leads to wastage of high resources, generation of scrap and off high time consuming. In order to overcome the problem faced, a methodology is developed and validated. The methodology is essentially a model-based approach for optimization of FSW process. The Figure3 presents a schematic representation of steps followed in overall methodology of model-based optimization of FSW process. In going forward with the objective, the first step was to develop FE model that can simulate FSW process and validate FE results with referring to various published research papers and results obtained from experimentation. The model was developed using ABAQUS-6.12 [10], that has a CEL formulation to simulate problems involving large deformations and is often difficult to solve using the classical FE Method. In the next step, simple optimization methods were used with goal of minimizing manufacturing costs and maximizing weld quality.

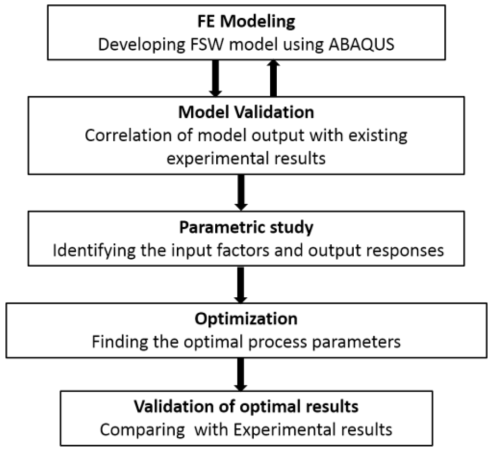

Figure3. Methodology of model-based optimization of FSW process

4. Model Description

FE model is developed in ABAQUS/Explicit using the Coupled Eulerian-Lagrangian Formulation, Johnson-Cook material law and Coulomb's Law of friction. The Coupled Eulerian-Lagrangian (CEL) method efforts to capture the strengths of Lagrangian and Eulerian methods. In general, a Lagrangian reference frame is used to discretize the Tool while an Eulerian frame is used to discretize the Work-piece [11-14]. Here the workpiece of 200 X 100 mm area and thickness of 5 mm is considered. The Eulerian domain is meshed with multi-material thermally coupled 8-node (EC3D8RT) Eulerian elements and the void region thickness is taken as 1 mm. The Johnson-Cook Johnson and Cook [15] equation (1) describes the flow stress as a product of the equivalent strain, strain rate, temperature dependent terms and several parameters to adequate the real behavior of the materials.

$$\sigma_y = \left[A + B\left(\varepsilon_p\right)^n\right]\left[1 + C\left(\frac{\varepsilon_p}{\varepsilon_o}\right)\right]\left[1 - \left(\frac{T - T_{room}}{T_{melt} - T_{room}}\right)^m\right] \quad (1)$$

where T_{melt} is the melting point or solidus temperature, T_{room} the ambient temperature, T the effective temperature, A the yield stress, B the strain factor, n the strain exponent, m the temperature exponent, $\varepsilon_p / \varepsilon_0$ the plastic strain and C the strain rate factor. A, B, C, n, and m are material/test constants for the Johnson-Cook strain rate dependent yield stress. The material properties of AA2024-T3, considered for simulations are as per the values taken by Veljic, et al. [16] and material constants for Johnson-cook are as per Mandal, et al. [17] and Hamilton, et al. [18].

The tool with shoulder and pin made of High density steel (HDS) material used in experiment is considered as rigid part and meshed with Lagrangian elements. The Figure4 shows schematic representation of dimensions of tool geometry.

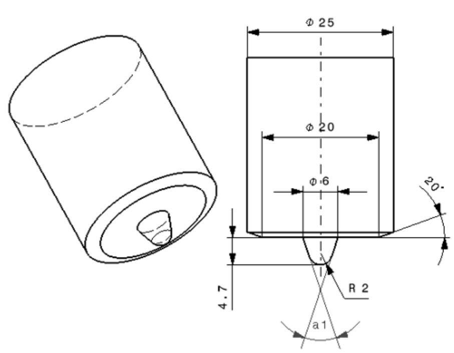

Figure4. Circular pin shaped frustum tool geometry

In ABAQUS, friction law used in solid mechanics and that suite for FSW modeling is modified Coulomb friction law [19, 20]. However for FSW the conventional Coulomb friction law will be only applied at the very beginning of welding when interface temperature is relatively low. As the interface plasticized material is formed in larger volumes at elevated temperatures, the friction behavior will be dominated by viscoplastic friction. Therefore, heat generation is dependent on intense plastic deformation of the thin shear layer at the interface [21]. A modified Coulomb friction law is then applied. Different values of Coefficient of Friction (COF) have been used in literature. Tutunchilar, et al. [22] used COF values of 0.4, 0.5 and 0.6, under 100 mm/min transverse speed and 900 rpm rotational speed. According to investigations made by Kumar, et al. [23] the COF and temperatures do have a synergic influence on each other. The COF in FSW condition was found to be as high as 1.2 to 1.4 in temperature range of 400-450°C. Therefore, in present simulations a friction coefficient of 1.0 is considered for all simulation conditions.

5. Model validation and parametric study

The model is developed referring to aluminium 2024 alloy experimental results. The validation is done using experimentally measured temperature, force on tool, torque, shape and size of weld zones and capability of predicting generation of defects. Also further validation of model was carried out using temperature results and macrographs published by Merzoug, et al. [24] and Hirasawa, et al. [25]. Here the results are categorized and discussed under sub sections. The welding parameters that are kept constant for different weld conditions during simulation and experiment are; Plunge velocity of 10 mm/min, Dwell Time of 10 sec, Plunge depth is 0.2 mm.

5.1 Effect of Coefficient of friction

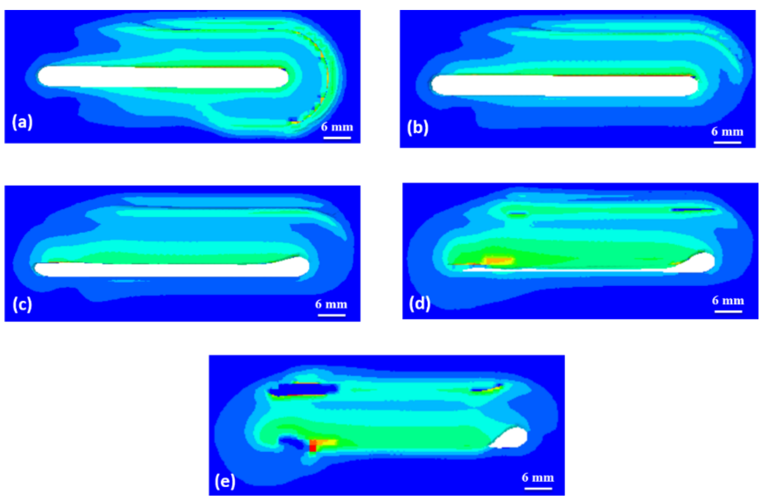

Figure 5. Effect of coefficient of friction on void size (Top view); (a) At μ= 0.2, (b) At μ = 0.4, (c) At μ = 0.6, (d) At μ = 0.8, (e) At μ = 1

The simulation results show that the coefficient of friction has a major effect on void formation, the lower the friction coefficient is applied, larger the void is formed. The Figure 5 shows the effect of coefficient of friction on void size at rotational speed of 1000 rpm. As the friction between tool and the workpiece increased the formation of void and moment of material was closer to that of experimental conditions. It can be seen that any value of $\mu < 1$ resulted in unrealistic prediction of results. Also considering $\mu > 1.2$ lead to over softening of material, which intern showed the defect as shown in Figure 6. For a sound weld, it is found from literature that the working temperature in FSW should be around 80% to 90% of melting temperature (Tmelt) of the welding material [26, 27]. The Figure 7 indicate that with μ =1, the maximum temperature predicted in simulation is in the intended range. In Figure 7 the percentage of error is calculated by considering the maximum temperature of 404.360C, recorded by thermocouple during the experiment. The resulted simulation temperature at μ =1 is in close agreement with thermocouple reading.

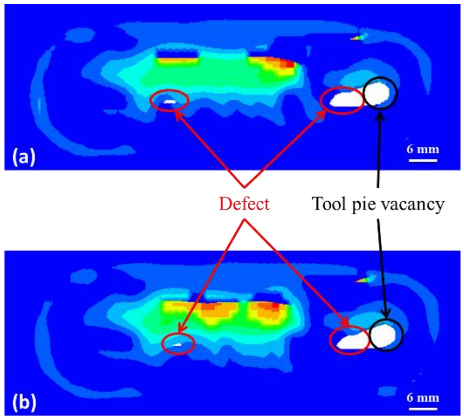

Figure 6. Effect of high coefficient of friction (Top view); (a) At μ = 1.4, (b) At μ = 1.6

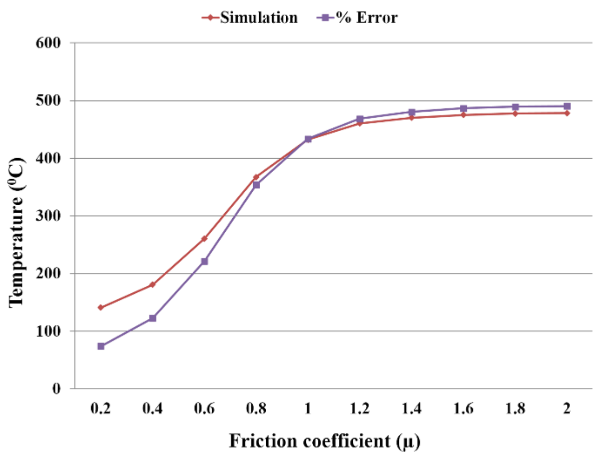

Figure 7. Simulation temperature with respect to friction coefficient

5.2 Temperature response

Plunge trials for temperature measurements were carried on AA2024-T3 (5 mm thick plate) with plunge velocity of 10 mm/min, 00 tilt and 0.2 mm plunge depth. Three trials were carried for tool rotational speeds of 350 rpm, 950 rpm and 1550 rpm each. The plunge and dwell phase was approximately of 30 and 10 seconds respectively. To measure the temperature change during experiments, thermocouples were employed. The mounting of thermocouples and the region in which the nodes are selected in simulations correspond to similar locations of thermocouples as illustrated in Figure 8. During plunge, gradual increase in temperature was observed for 350 rpm unlike 950 and 1550 rpm (see Table 1). It is observed that temperature reaches a steady state in dwell phase of the weld as shown in graphs (see Figure9). This points to the fact that temperature has linear relation with plunge depth; it increases with increase in plunge depth and vice-versa. For a given plunge depth there is a certain maximum temperature that can be obtained and once it is achieved it remains the same in dwell phase too. The Figure 8(a) shows the close-up view of temperature profile after plunge and dwell phase on the top sheet. Left column shows the images from experiments and right column exhibits simulation images with predicted temperature.

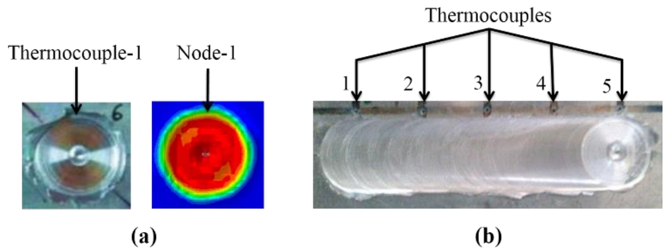

Figure 8. Location of thermocouples in experiment and simulation.

Table 1. Comparison between numerically estimated and experimentally measured temperature

	Temperature (^{0}C)		
Tool rotation (rpm)	**Experimental**	**FEM**	**Error %**
350	326.64	349.98	7.15
650	369.14	392.56	6.34
950	404.36	432.14	6.87
1250	435.43	454.79	4.45
1550	475.13	489.63	3.05
Average			**5.57**

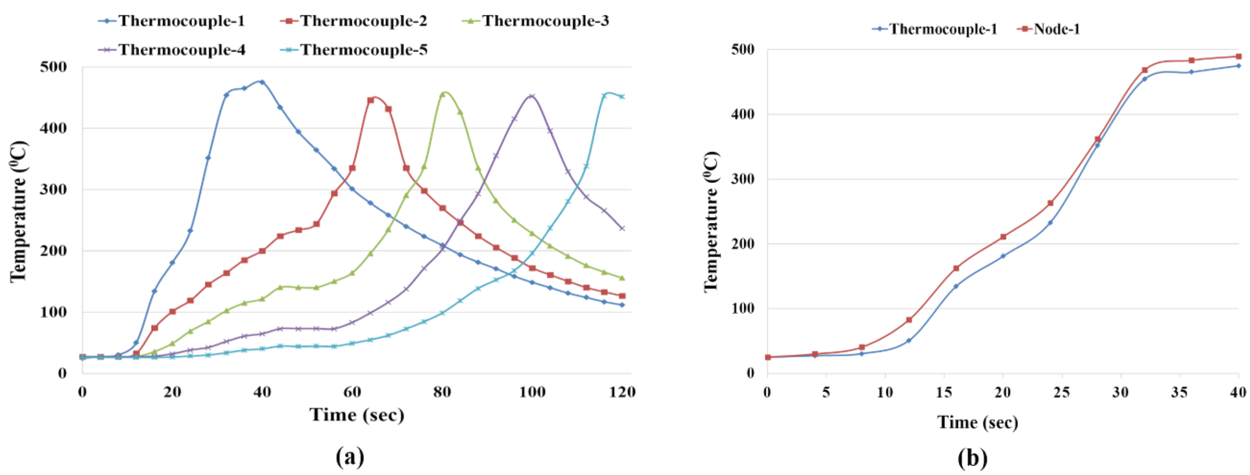

Figure9. (a) Temperature measured during plunge, dwell and traverse in experiment at 1550rpm, (b) Comparison simulation readings for plunge and dwell phase

5.3 Defect prediction

The developed model is capable of predicting the formation of defects for a set of process parameters. It gives the close representation of external defects as shown in Figure10 and also internal defects as shown in Figure11 when compared with experimental images. The results show that a defect is generated for lower rotational speed and it reduces as the rotational speed increases. The same effects were observed in the study conducted on Al 6061 sheets by Ramulu, et al. [28].

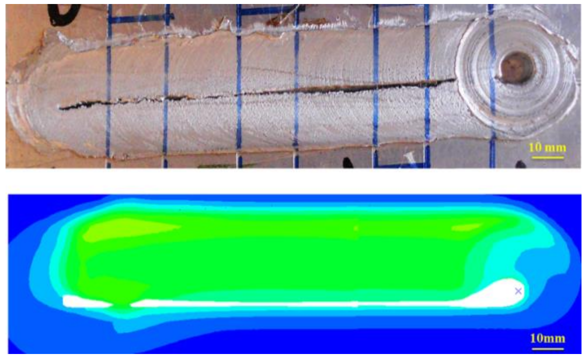

Figure10. Formation of external defect at 200 rpm with tool tilt angle of 0^0

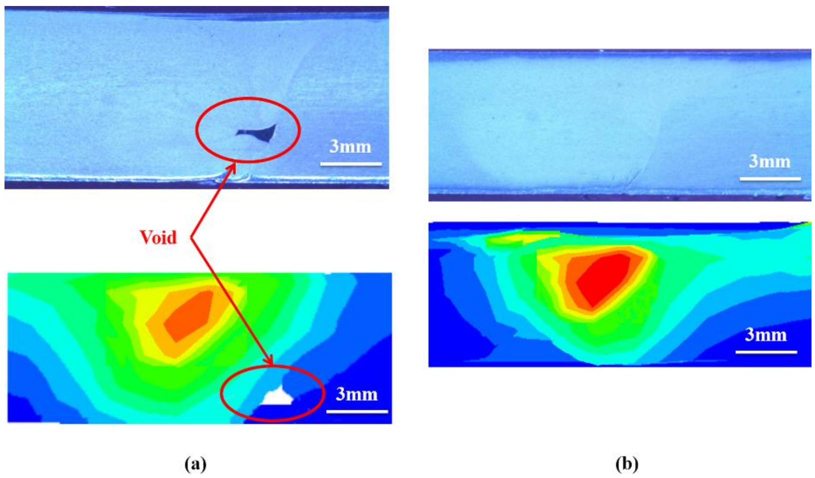

Figure11. (a) Void Formation at 600 rpm with tool tilt angle of 0^0 (b) Defect free weld at 1000 rpm with tool tilt angle of 0^0

The results showed that the increase of the rotational speed and the decrease of the welding speed can improve the friction stir weld quality, but flash formation would be more obvious when rotational speed is increased more and decreased welding speed leads to higher weld time. The model capability of predicting the generation of various defects that accrue in FSW due to various parameters can also be predicted. The Figure 12 shows comparison of various defect accrued in physical welding to simulation prediction. The actual size of defect, material and parameters are not exactly matches with the simulation conditions. Here the images are only compared to show the capability of model in predicting the generation of various defects by modeling.

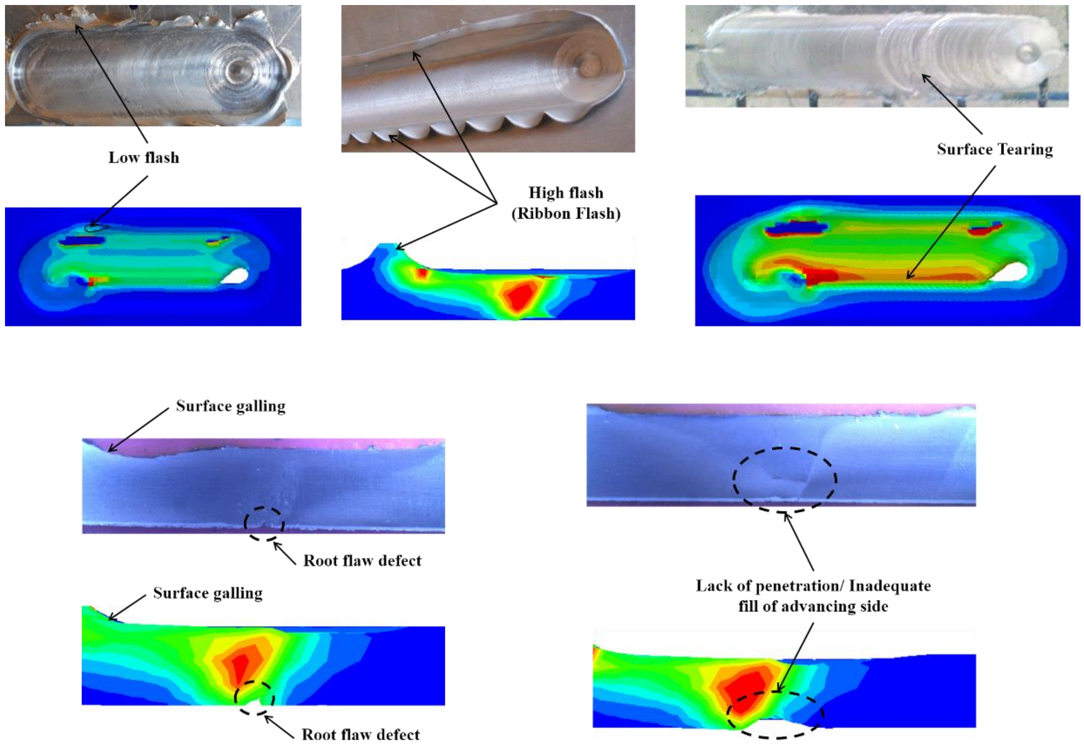

Figure 12. Comparison of various defect accrued in physical welding to simulation prediction

5.4 Simulation time

The time taken for simulation as stated by Lasley [29] is 42 days to run 5.44 seconds of simulation using supercomputing facility and as stated from Awang [30] it is 14 days and 12 hours on a 3.60 GHz Intel Pentium 4 processor for the simulation time of 1.505 seconds. With further advancements in FE packages there was as a little reduction in computational time. As stated from Assidi, et al. [31] it is 12 days 20 hours with ALE formulation and 6 days 14 hours with Eulerian formulation. But in present work, with the use of CEL the time taken for simulation is greatly reduced. It is 9.5 hours with core 2 duo processor and 4.5 hours with i7 processor. Also the high distortion and convergence problems with Lagrangian and ALE formulations are overcome.

6. Process Parameters Optimization

FSW process operation in general can also be optimized by obtaining optimal values for parameters such as tool rotational speed, axial force, traverse speed, tool dimension, temperature, stress-strain, strain rate, defects and other parameters such as force on tool and stress in tool as well as in fixtures. Several optimization techniques could be applied to optimize FSW models. However, as the FSW is relatively new technology, there have been only a few attempts to use mathematical optimization techniques to optimize the process. Here, a basic level of optimization is done to show the capability of the results obtained from FE model for a given application.

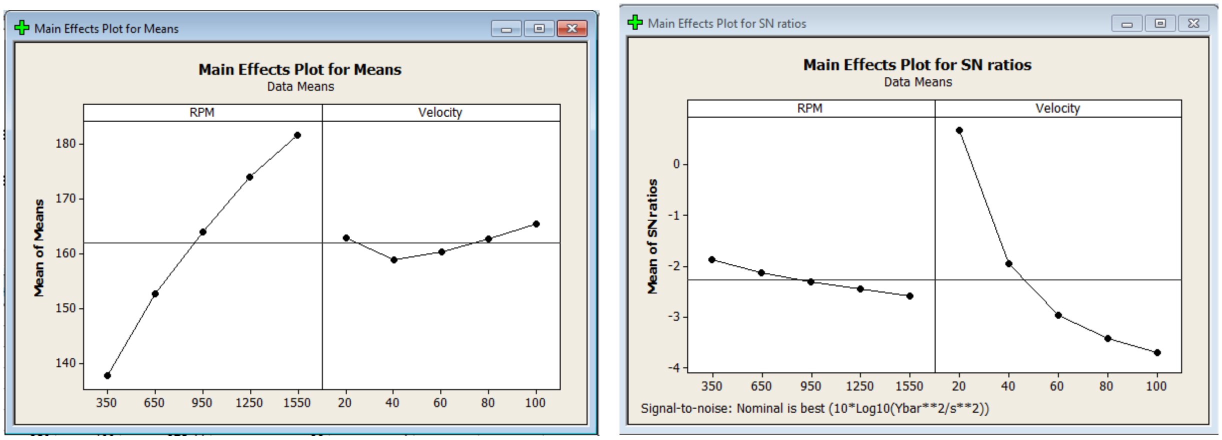

(a) (b)

Figure13. (a) Main Effect Plot for means and (b) Main effect plots for S/N ratios

Worksheet 3 ***

↓	C5	C6	C7	C8
	RPM	Velocity	Temperature	Wlding time (sec)
1	950	20	300.62	180
2	950	100	465.19	36
3	1550	60	475.41	60
4	950	60	425.23	60
5	350	60	349.78	60
6	1550	20	356.87	180
7	350	100	375.44	36
8	950	60	425.23	60
9	950	60	425.23	60
10	1550	100	512.64	36
11	950	60	425.23	60
12	950	60	425.23	60
13	350	20	251.82	180
14				
15				

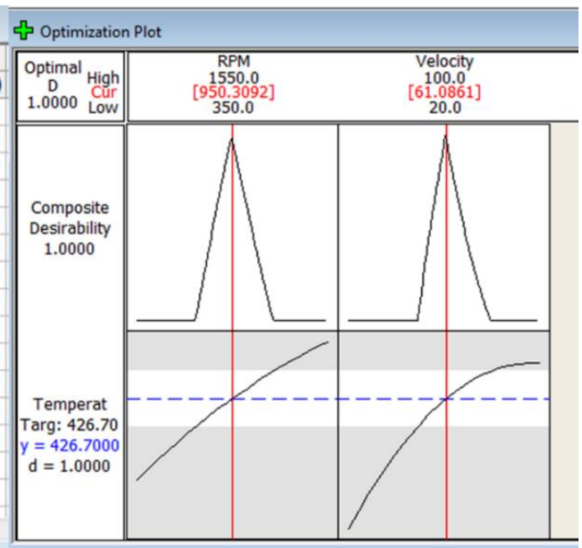

Figure14. Appropriate value of each factor which effect to temperature (optimization plot)

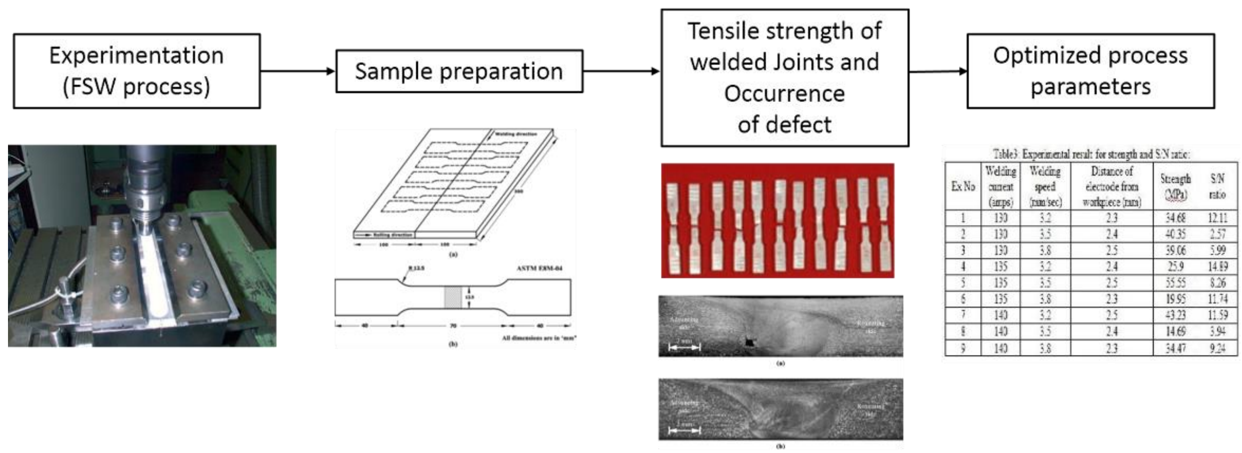

(a)

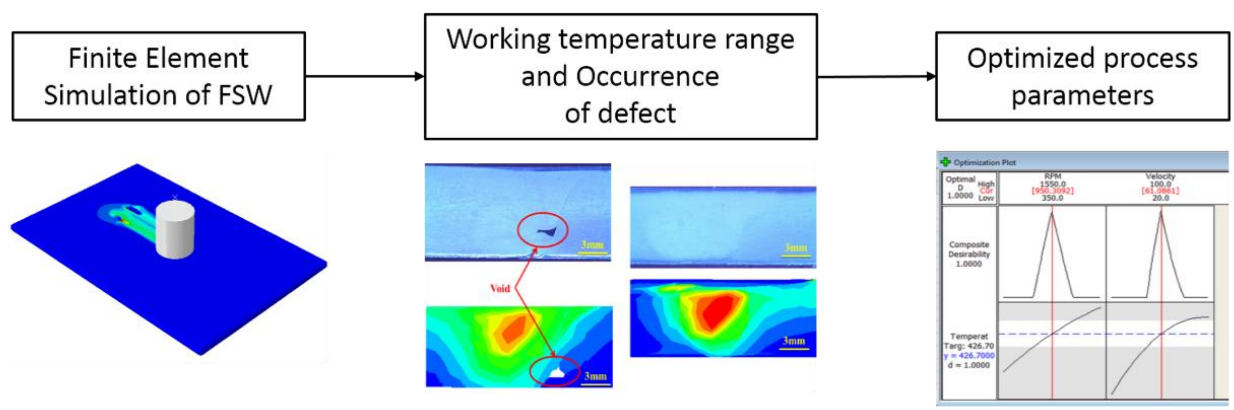

(b)

Figure15. Process parameters optimization procedures: (a) Experimental bases procedure, (b) FE modeling based procedure

With the data obtained from the simulated model, Taguchi and the Response surface optimization techniques were carried out using MINITAB [32]. The optimization process is based on defects observed, welding time taken and optimal temperature range, with tool rotation and weld velocity as variables. Here, with the results of Taguchi and Response surface optimization techniques obtained from MINITAB (Figure13 and Figure14), optimized process parameters predicted were 950 rpm (tool rotation) with 60 mm/min (weld velocity). There was a good correlation with experiment and simulation at these parameters. This shows in a border sense, the capability of results obtained from FE model in performing optimization. The Figure15 (a) shows the schematic representation of experimental based procedure of obtaining optimized process parameters and Figure15 (b) shows the FE modeling based procedure of obtaining optimized process parameters in FSW. It can be visualized that FE modeling based technique takes lesser time and eliminates experimentation, material and tooling costs.

7. Challenges

Four major challenges had been addressed while solving the present problem. The first challenge was to develop a FE model using ABAQUS which closely simulates the actual process. This involved the selection of proper formulation, material model and boundary conditions. The second one was to predict the parameters leading to defect and defect free welds. The third one was to accomplish the objective in minimum possible simulation time to make this approach effective and efficient and the fourth, to obtain optimal process parameters with simple optimization method and validate with experimentation.

8. Conclusions

Based on the investigations carried out in the present research and the results obtained, following conclusions can been made:

(i) Based on the comparison of the simulation and experimental results, under the no slip condition (μ=1) and Johnson-Cook material model in ABAQUS/Explicit environment, the proposed model is capable of predicting right processing parameters.
(ii) CEL method exhibited the greater potential of defect prediction in FSW for given process conditions which ultimately can help in selecting the appropriate process parameters prior to performing welding process. It also helps in reducing simulation time to a larger extent thereby making FE simulations of FSW economical.
(iii) Prediction of defects, temperature profile, stress strain profile and mainly optimizing the process parameters using FE modeling of FSW would greatly help in widening the applicability of FSW practice.
(iv) The proposed FE modeling method comprehended the possibility of obtaining the optimized process parameters and presented the strong possibility of widening the effective optimization study on FSW and its variants.

9. References

[1] ir. Kevin Deplus. (2014). *ALUWELD : Innovative welding of aluminium alloys – Hybrid Laser Welding and Friction Stir Welding*.
[2] Sanjeev N.K, Vinayak Malik, and H. Suresh Hebbar, "Effect of Coefficient of Friction in Finite Element Modeling of Friction Stir Welding and its Importance in Manufacturing Process Modeling Applications," *International Journal of Applied Sciences and Engineering Research, Vol. 3, No. 4, 2014* vol. 3, pp. 755-762, 2014.
[3] R. S. Mishra and Z. Y. Ma, "Friction stir welding and processing," *Materials Science and Engineering: R: Reports,* vol. 50, pp. 1-78, 2005.
[4] Rajiv S. Mishra and Murray W. Mahoney, *Friction Stir Welding and Processing*: ASM International, 2007.
[5] K. Kumar and Satish V. Kailas, "On the role of axial load and the effect of interface position on the tensile strength of a friction stir welded aluminium alloy," *Materials & Design,* vol. 29, pp. 791-797, 2008.
[6] K. Kumar, Satish V. Kailas, and T. S. Srivatsan, "Influence of Tool Geometry in Friction Stir Welding," *Materials and Manufacturing Processes,* vol. 23, pp. 188-194, 2008.
[7] Vinayak Malik, Sanjeev N K, H. Suresh Hebbar, and Satish V. Kailas, "Time Efficient Simulations of Plunge and Dwell Phase of FSW and its Significance in FSSW " in *International Conference on Advances in Manufacturing and Materials Engineering*, NITK, Surathkal, 2014.
[8] Sanjeev N K, Vinayak Malik, and H. Suresh Hebbar, "Verification of Johnson-Cook Material Model Constants 0f AA2024-T3 for use in Finite Element Simulation of Friction Stir Welding and its Utilization in Severe Plastic Deformation Process Modelling," *International Journal of Research in Engineering and Technology,* vol. 3, pp. 98-102, 2014.
[9] R. K. Uyyuru and Satish V. Kailas, "Numerical Analysis of Friction Stir Welding Process," *Journal of Materials Engineering and Performance,* vol. 15, pp. 505-518, 2006.
[10] "ABAQUS Version 6.12, User Documentation, Dassault Systems," 2012.
[11] Kevin H. Brown, Shawn P. Burns, and Mark A. Christon, "Coupled Eulerian-Lagrangian Methods for Earth Penetrating Weapon Applications," *Sand Report,* pp. Sand2002-1014, 2002.
[12] Benson D.J, "Computational Methods in Lagrangian and Eulerian Hydrocodes," vol. 99, pp. 235-394, 1992.
[13] Karim H. Muci-Küchler, Sindhura Kalagara, and William J. Arbegast, "Simulation of a Refill Friction Stir Spot Welding Process Using a Fully Coupled Thermo-Mechanical FEM Model," *Journal of Manufacturing Science and Engineering,* vol. 132, p. 014503, 2010.
[14] User Documentation, "ABAQUS Version 6.12," *Dassault Systems,* 2012.

[15] Gordon R. Johnson and William H. Cook, "A Constitutive Model and Data for Metals Subjected to Large Strains, High Strain Rates and High Temperatures, ," *Proceedings, 7th International Symposium on Ballistics, Hague, The Netherlands,* pp. 541-547, 1983.

[16] Darko M. Veljic, Marko P. Rakin, Milenko M. Perovic, Bojan I. Medjo, Zoran J. Radakovic, Petar M. Todorovic, *et al.*, "Heat Generation During Plunge Stage In Friction Stir Welding," *Thermal Science,* vol. 17, pp. 489-496, 2013.

[17] S. Mandal, J. Rice, and A. A. Elmustafa, "Experimental and numerical investigation of the plunge stage in friction stir welding," *Journal of Materials Processing Technology,* vol. 203, pp. 411-419, 2008.

[18] Robert Hamilton, Donald MacKenzie, and Hongjun Li, "Multi-physics simulation of friction stir welding process," *Engineering Computations,* vol. 27, pp. 967-985, 2010.

[19] Olivier Lorrain, Jérôme Serri, Véronique Favier, Hamid Zahrouni, and Mourad El Hadrouz, "A Contribution To A Critical Review Of Friction Stir Welding Numerical Simulation," *Journal Of Mechanics Of Materials And Structures,* vol. 4, pp. 351-370, 2009.

[20] H. Schmidt, J. Hattel, and J. Wert, "An analytical model for the heat generation in friction stir welding," *Modelling and Simulation in Materials Science and Engineering,* vol. 12, pp. 143-157, 2004.

[21] Wenya Li, Zhihan Zhang, Jinglong Li, and Y. J. Chao, "Numerical Analysis of Joint Temperature Evolution During Friction Stir Welding Based on Sticking Contact," *Journal of Materials Engineering and Performance,* vol. 21, pp. 1849-1856, 2011.

[22] S. Tutunchilar, M. Haghpanahi, M. K. Besharati Givi, P. Asadi, and P. Bahemmat, "Simulation of material flow in friction stir processing of a cast Al–Si alloy," *Materials & Design,* vol. 40, pp. 415-426, 2012.

[23] K. Kumar, C. Kalyan, Satish V. Kailas, and T. S. Srivatsan, "An Investigation of Friction during Friction Stir Welding of Metallic Materials," *Materials and Manufacturing Processes,* vol. 24:4, pp. 438-445, 2009.

[24] Mohamed Merzoug, Mohamed Mazari, Lahcene Berrahal, and Abdellatif Imad, "Parametric studies of the process of friction spot stir welding of aluminium 6060-T5 alloys," *Materials & Design,* vol. 31, pp. 3023-3028, 2010.

[25] Shigeki Hirasawa, Harsha Badarinarayan, Kazutaka Okamoto, Toshio Tomimura, and Tsuyoshi Kawanami, "Analysis of effect of tool geometry on plastic flow during friction stir spot welding using particle method," *Journal of Materials Processing Technology,* vol. 210, pp. 1455-1463, 2010.

[26] Jinwen Qian, Jinglong Li, Fu Sun, Jiangtao Xiong, Fusheng Zhang, and Xin Lin, "An analytical model to optimize rotation speed and travel speed of friction stir welding for defect-free joints," *Scripta Materialia,* vol. 68, pp. 175-178, 2013.

[27] Yuh J. Chao, X. Qi, and W. Tang, "Heat Transfer in Friction Stir Welding—Experimental and Numerical Studies," *Journal of Manufacturing Science and Engineering,* vol. 125, p. 138, 2003.

[28] P. Janaki Ramulu, R. Ganesh Narayanan, Satish V. Kailas, and Jayachandra Reddy, "Internal defect and process parameter analysis during friction stir welding of Al 6061 sheets," *The International Journal of Advanced Manufacturing Technology,* vol. 65, pp. 1515-1528, 2012.

[29] Mark Jason Lasley, "A finite element simulation of temperature and material flow in fricton stir welding," Master of Science, School of Technology, Brigham Young University, United States, 2005.

[30] Mokhtar Awang, "Simulation of Friction Stir Spot Welding (FSSW) Process: Study of Friction Phenomena," 2007.

[31] Mohamed Assidi, Lionel Fourment, Simon Guerdoux, and Tracy Nelson, "Friction model for friction stir welding process simulation: Calibrations from welding experiments," *International Journal of Machine Tools and Manufacture,* vol. 50, pp. 143-155, 2010.

[32] "Minitab 17 Documentation," 2014.

APPENDIX

Johnson-Cook constants and material properties of AA2024-T3

Material constants for Johnson-cook						
A (MPa)	B (MPa)	n	C	m	T_{melt} (°C)	T_{ref}
369	684	0.73	0.0083	1.7	502	25

Material properties						
Temp (°C)	Density Kgm^{-3}	Young's modulus (GPa)	Yield stress (MPa)	Thermal conductivity ($Wm^{-1}K^{-1}$)	Specific heat capacity ($Jk^{-1}g°C^{-1}$)	Coefficient of thermal expansion (10^{-6} °C^{-1})
25	2785	73.1	345	175	875	24.7
100	2770	71.5	335	185	897	25.2
200	2750	68.4	315	194	922	26.4
300	2730	64.7	295	191	952	28.7
400	2707	60.2	265	190	987	30.9
500	2683	55.8	125	188	1002	31.6
538	2674	49.3	75	184	1023	32.1
638	2500	42.3	25	85	1054	33.5

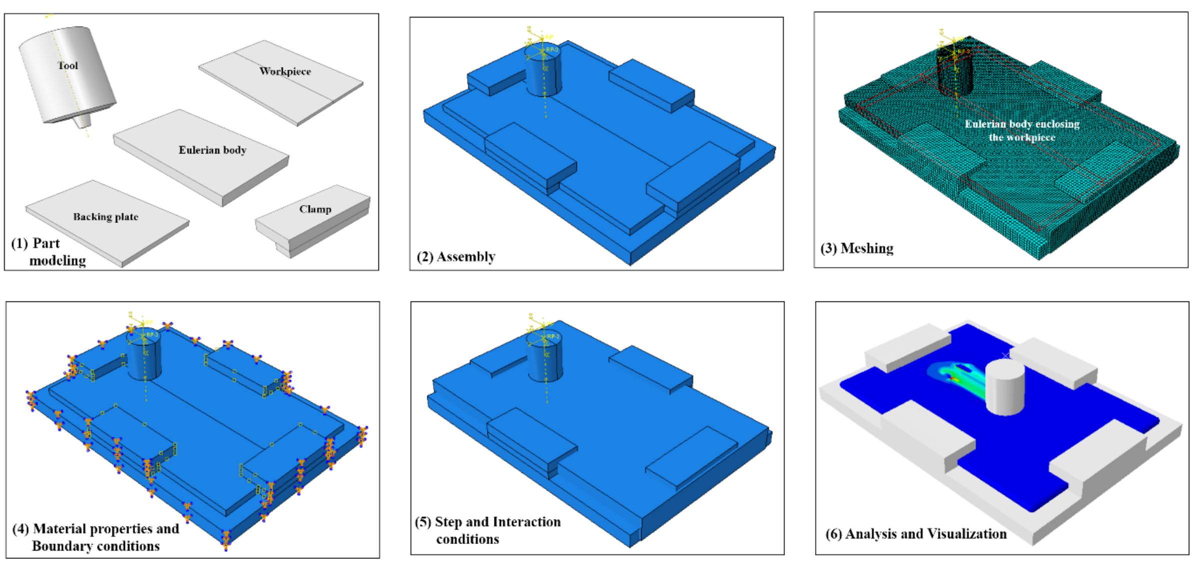

FSW Modeling Steps in ABAQUS Environment

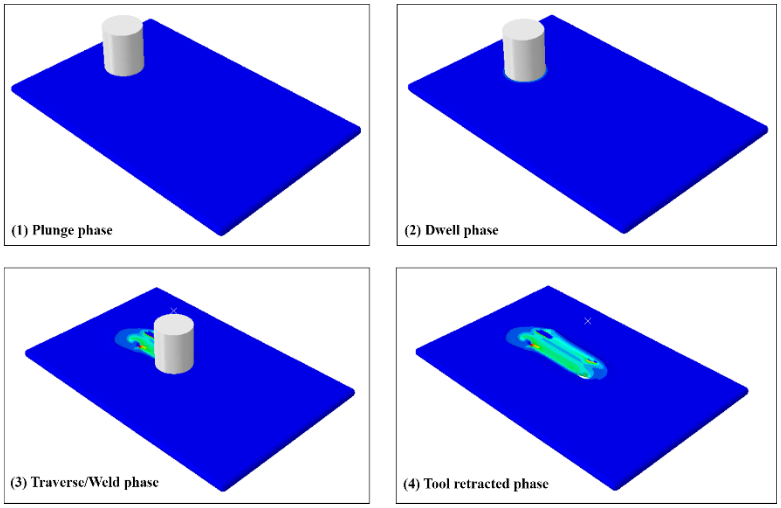

FSW Phases as Visualized in Developed FE Model

Simulation results with respect tool rotation and weld speed

Inputs		Outputs		
Simulation results with respect tool rotation and weld speed Tool rotation (rpm)	Weld speed (mm/min)	Temperature (°C)	Welding time (sec)	Observation (Defect types)
350	20	251.82	180	Visible defect
650	20	272.64	180	Visible defect
950	20	300.62	180	Visible defect
1250	20	339.66	180	Visible defect
1550	20	356.87	180	Visible defect
350	40	301.39	90	Visible defect
650	40	363.21	90	Visible defect
950	40	390.56	90	Internal defect
1250	40	411.52	90	Defect Free
1550	40	451.96	90	Defect Free
350	60	349.78	60	Visible defect
650	60	388.56	60	Internal defect
950	60	425.23	60	Defect Free
1250	60	454.79	60	Defect Free
1550	60	475.41	60	Defect Free
350	80	360.54	45	Visible defect
650	80	409.76	45	Defect Free
950	80	452.87	45	Low flash
1250	80	475.41	45	Low flash
1550	80	503.43	45	High flash
350	100	375.44	36	Internal defect
650	100	430.21	36	Low flash
950	100	465.19	36	Low flash
1250	100	502.11	36	High flash
1550	100	512.64	36	High flash